Electrical power free, low dead volume, pressure-driven pumping for microfluidic applications

Mario Moscovici,[1,2] Wei-Yin Chien,[2] Mohamed Abdelgawad,[1,3,a)] and Yu Sun[1,2,b)]
[1]*Department of Mechanical and Industrial Engineering, University of Toronto, 5 King's College Rd., Toronto, Ontario M5S 3G8, Canada*
[2]*Institute of Biomaterials and Biomedical Engineering, University of Toronto, 164 College St., Toronto, Ontario M5S 3G9, Canada*
[3]*Department of Surgery (Urology), University of Toronto, 100 College Street, Toronto, Ontario M5G 1L5, Canada*

(Received 19 July 2010; accepted 21 September 2010; published online 13 October 2010)

This paper presents a simple-to-construct, low dead volume pump capable of generating a wide range of positive and negative pressures for microfluidic applications. The pump generates pressure or vacuum by changing the volume of air confined inside a syringe and is able to generate pressures between −95 and +300 kPa with a resolution as high as 1 Pa. Different from syringe pumps and electrokinetic pumping, which are capable of controlling flow rates only, our pump can be used to generate constant flow rates or constant pressures, which are required for certain applications such as the aspiration of biological cells for biophysical characterization. Compared to syringe pumps, the new pump has almost zero dead volume and does not exhibit pulsatile flows. Additionally, the system does not require electrical power and is cost effective (~$100). To demonstrate the capabilities of the pump, we used it to aspirate osteoblasts (MC3T3-E1 cells) and to determine Young's modulus of the cells, to generate a concentration gradient, and to produce variable-sized droplets in microchannels using hydrodynamic focusing. © *2010 American Institute of Physics.* [doi:10.1063/1.3499939]

I. INTRODUCTION

Pumping is indispensable for microfluidic applications, such as culturing cells inside microchannels,[1] separating a mixture of analytes,[2] amplifying DNA fragments,[3] sorting cells[4] or isolating them,[5] controlling drug delivery to individual cells,[6] or synthesizing particles inside microchannels.[7] Consequently, the development of pumps has received and will continue to receive significant attention in microfluidic research.

The various pumping methods in microfluidics can be classified into on-device pumps and external pumps. In the former category, micropumps are integrated in the microfluidic device and are fabricated with the device itself. This category includes piezoelectric, thermal, electrohydrodynamic, electrostatic, rotary, and acoustic micropumps, among others.[8] Although on-device pumps increase device portability, integrating pumping components (e.g., diaphragms, actuators, valves, and heaters) on the device significantly increases fabrication complexity and device cost. Since most microfluidic devices are made to be disposable to reduce contamination across samples, on-device pumping is not always an attractive choice.

The second category, external pumping, includes mainly electro-osmotic pumping and syringe

[a)]Currently with the Mechanical Engineering Department, Assiut University, Egypt.
[b)]Author to whom correspondence should be addressed. Department of Mechanical and Industrial Engineering, Institute of Biomaterials and Biomedical Engineering, University of Toronto, 5 King's College Road, Toronto, ON M5S 3G8, Canada. Tel.: 416-946-0549. FAX: 416-978-7753. Electronic mail: sun@mie.utoronto.ca.

pumps. Electro-osmotic pumping exploits ions accumulated in the electric double layer when a liquid comes into contact with channel walls. When an electric field is applied between two electrodes in the channel inlet and outlet reservoirs on the device, the ions in the electric double layer are attracted toward the opposite polarity electrode, hence inducing a net flow in the microchannel.[9] Electro-osmotic pumping can induce and control the flow with no moving parts; however, it suffers from bubble generation due to electrolysis at the electrodes, which may cause channel blockage. Moreover, electro-osmotic flow requires high voltages (e.g., kilovolts) to induce significant flow rates, which can result in significant Joule heating. Expensive high-voltage sequencers are typically used for electro-osmotic pumping, increasing the complexity and capital cost associated with the setup.

Syringe pumps are relatively cheaper compared to electro-osmotic pumping setups. However, they involve large dead volumes in the syringe and tubing. This large dead volume compromises the advantage of reduced sample and reagent consumption in microfluidic devices. In addition, syringe pumps are prone to producing pulsatile flows at low flow rates.[10]

This paper reports a simple-to-construct system for pumping liquids in microchannels. The pump relies on pressure rather than forced displacement to drive liquids in microchannels. This technique was previously used in stop-flow lithography[11] using external pressure sources and regulators. Pressure-driven pumping was also implemented using electrolysis gases produced on-chip,[12,13] a pressurized gas in a microcavity,[14] and capillary pressure inside microdroplets.[15] In our pumping system, pressure is produced by changing the volume of air confined inside a syringe, which is simpler and more predictable compared to the aforementioned pressure-driven methods. Besides the capability of producing positive pressures, our method is also capable of producing vacuum, which is useful in some applications such as bubble elimination.[16] Moreover, using pressure to drive liquids in microchannels results in almost zero dead volume and does not exhibit pulsatile flows, which are two limitations of conventional syringe pumps. To demonstrate the effectiveness and versatility of our proposed pumping system, we demonstrated its usage in several microfluidic applications, including micropipet aspiration of biological cells, droplet generation in microchannels, and the generation of a concentration gradient.

II. EXPERIMENTAL METHODS

A. System setup

The pump consists of a plastic syringe connected to a microfluidic device (via 1/16 in. Tygon tubing) through an intermediate tank, which controls the initial system volume and thus changes pressure resolution and range [Fig. 1(a)]. Different syringe sizes can be used to allow for course or fine tuning of the pressure. We used two 60 ml plastic syringes as a variable size tank to allow for a wide range of resolutions from the same setup by tuning the tank volume. However, larger or smaller containers can be used to further increase the resolution or pressure range, respectively. Syringes were mounted on an off-the-shelf threaded corner-clamp to facilitate fine changes to syringe volume. The clamp also helps hold the syringe plunger in its place against generated pressure/vacuum for steady pressure generation. Tubing was connected to syringes via barbed-luer connection adapters (McMaster-Carr, Atlanta, GA) to allow for fast assembly/disassembly. A luer connection valve was added to the system to enable fast system venting. An optional pressure sensor (D1-4V 10 INCH, $100, All Sensors, Morgan Hill, CA) was incorporated into the system to measure the actual generated pressures and compare it with theoretically predicted values.

B. Pump operation

To achieve certain pressure range for a particular application, first the tank volume is chosen according to the analysis in the results section. Generally speaking, a smaller tank volume corresponds to larger pressure range and vice versa. In the setup shown in Fig. 1(a), two 60 ml syringes are used as a tank to have the ability to change tank volume without the need of changing the tank itself. Second, a proper syringe size is chosen to achieve the required resolution, which depends on the size of the smallest division on the syringe relative to the tank volume (the smaller the syringe

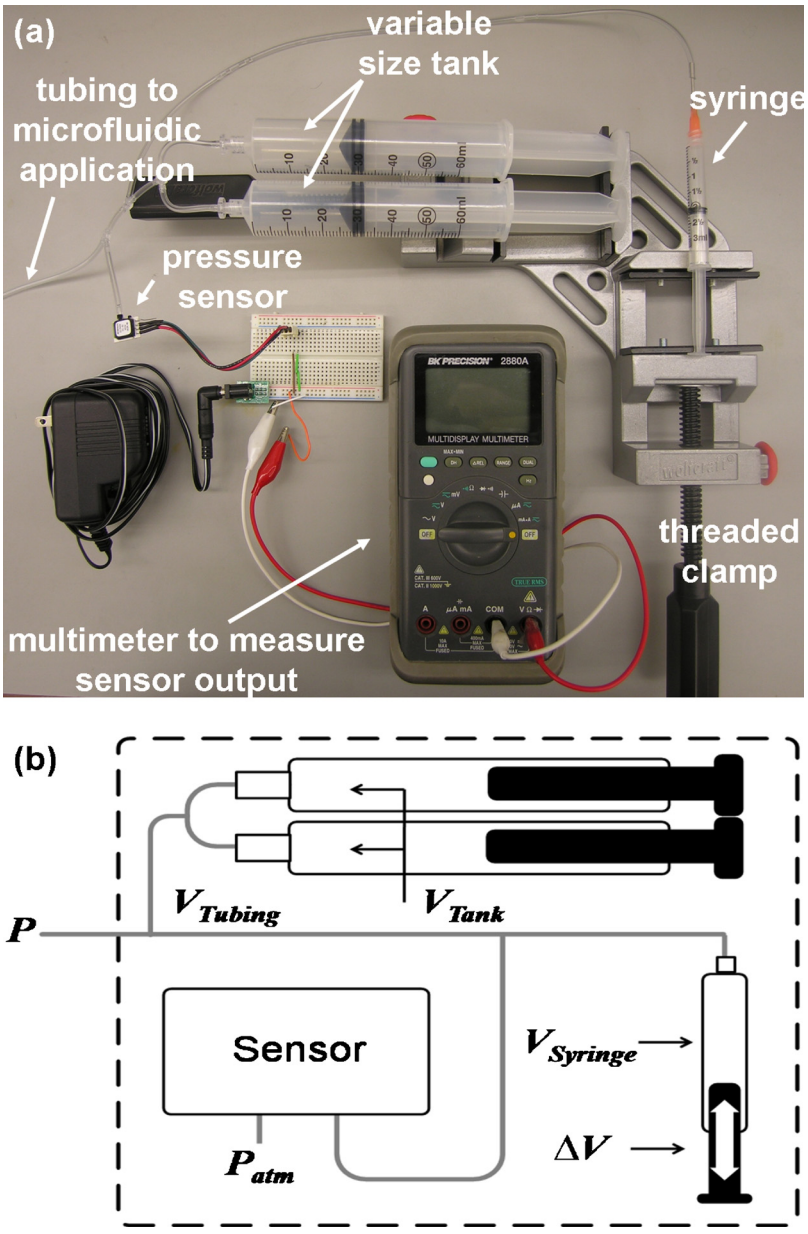

FIG. 1. (a) Picture of the pumping system with a pressure sensor included for system characterization. Two 60 ml syringes were used as a tank to allow for easy changes in tank volume. However, larger/smaller containers can be used as a tank to increase range/resolution, respectively. The pressure sensor (powered using a standard 5 V adapter through a bread board) is optional and was used to compare generated pressures with theoretical calculations. Sensor output span was 4 V (linearly proportional to pressure) and was measured using a conventional multimeter. (b) Working principle with variables used in Eq. (2).

volume, the higher the resolution; see Sec. III for a complete analysis). Since resolution is also dependent on tank volume, a compromise between high range and high resolution exists. After the proper syringe and tank sizes are chosen, the syringe is mounted on the threaded clamps and is connected to the tank via 1/16 in. tubing as shown in Fig. 1(a). Rotating the knob where the syringe is mounted causes the volume in the system to change in small increments, ΔV in Fig. 1(b), which consequently changes the pressure of the system. If pressure needs to be measured, a

pressure sensor can be connected to the system. Sensor output, in volts, is measured using a multimeter and converted into pressure according to sensor characteristics.

C. Flow measurements

For flow rate measurements, the syringe plunger position was set to generate certain vacuum pressure according to the analysis given in Sec. III. The actual generated vacuum was measured using the pressure sensor and was used to pump 1 μm diameter FITC fluorescent beads (Bangs Laboratories, Fishers, IN) suspended in methanol (μ=0.58 mPa S) inside a microchannel (140 μm wide, 25 μm high, and 30 mm long). The speed of the FITC beads was measured by increasing the exposure time to visualize streaks of the beads as they flow in the channel. Speed was calculated by dividing the streak length by the exposure time. Average flow rate was calculated from the maximum speed at the channel centerline using the following equation[17] for channels with height to width ratio $\alpha < 0.5$:

$$\frac{u}{u_{\mathrm{av}}} = \left(\frac{m+1}{m}\right)\left(\frac{n+1}{n}\right)\left[1-\left(\frac{y}{b}\right)^{n}\right]\left[1-\left(\frac{z}{a}\right)^{m}\right], \tag{1}$$

where u is liquid velocity at any location in the channel, u_{av} is average liquid velocity, b is the channel height, a is the channel width, y and z are the two coordinates measured from channel centerline along channel height and width, respectively, and m and n are two numerical factors calculated according to

$$m = 1.7 + 0.5\ \alpha^{-1.4}, \tag{2}$$

$$\begin{cases} n = 2 & \alpha < 1/3 \\ n = 2 + 0.3(\alpha - 1/3) & \alpha \geq 1/3. \end{cases} \tag{3}$$

D. Micropipet aspiration of osteoblasts

Conventional micropipet aspiration experiments were conducted on osteoblasts (MC3T3-E1) cells using the proposed pump to verify its capacity for high resolution vacuum generation. A borosilicate glass micropipet tip (5 μm diameter) was held by a micromanipulator (Sutter Instrument Co., CA, USA) mounted on an inverted phase-contrast microscope. The micropipet was connected (via 1/16 in. tubing) to the pump where the tank volume used was 120 ml and a 1 ml syringe with visible divisions of 0.01 ml was used to generate the vacuum. The resolution generated from the setup was 8 Pa with a range of 0–(−730) Pa.

First, the micropipet tip was immersed inside a droplet of culture media with no cells for a few minutes to stabilize capillary rise into the pipet tip. A second droplet of culture medium with cells was added to the droplet after the system was stabilized. Then, the tip was positioned close to the surface of a target cell, and a small negative pressure (20–50 Pa) was applied in order to immobilize the cell and to form a complete seal. From this reference state, subsequent suction pressures, in increments of 16 Pa, were then applied and images of the aspirated cell were captured from which the aspiration length and pipet diameter were measured. Young's modulus values of the aspirated cells were determined by using common biomechanics models that approximate the cell as an elastic half-space solid.[18,19]

E. Concentration gradient

To generate a concentration gradient, red and green food dyes were loaded into the inlet reservoirs of a gradient generator device.[20] A vacuum pressure of 15 kPa (tank size=11 ml and syringe displacement=2 ml) was applied at the outlet, pulling the two dyes through the branches of the microchannel network and resulting in a seven-step concentration gradient at the outlet channel.

F. Droplet generation

Water droplets (aqueous phase) were generated in a continuous phase of silicone oil (DMS-T01, viscosity=1 cSt., Gelest, Inc., Morrisville, PA) using a hydrodynamic focusing device similar to one reported previously.[21] First, the whole device was filled with silicone oil, and a pressure of 20 kPa (V_{total}=60 ml and plunger displacement=−10 ml) was applied on the two side reservoirs to generate oil flow in the downstream channel. Water was then added to the center channel reservoir, and a pressure of 100 kPa (V_{total}=60 ml and plunger displacement=−30 ml) was therein applied to generate a stream of water along the center of the downstream channel. Tween 20 (Sigma-Aldrich, Oakville, ON) can be added to the water stream as a surfactant, at low concentrations (e.g., 1.75% v/v), to facilitate breaking of the water-oil interface. Oil flow rate in the side channels was then increased by increasing the applied pressure on oil reservoirs to 114 kPa (V_{total}=60 ml and plunger displacement=−32 ml) to pinch the water stream into discrete droplets. Smallest droplet size (see results section) was achievable with a pressure of 300 kPa (V_{total}=60 ml and plunger displacement=−45 ml) applied on the oil reservoirs.

III. RESULTS AND DISCUSSION

Any change in the volume of a confined gas produces a change in its pressure according to the equation of state. Assuming an isothermal process, the change in pressure of an ideal gas is inversely proportional to its volume according to

$$PV = C, \tag{4}$$

where P is the absolute pressure, V is the volume of the confined gas, and C is a constant that can be calculated from the initial pressure and volume values. Assuming that the initial volume of our system is V_{total}, which comprises the volume of the tank, the tubing, and initial volume on the syringe ($V_{total}=V_{tank}+V_{tubing}+V_{syringe,initial}$), and that the initial pressure is atmospheric pressure (P_{atm}), then the gauge pressure of the system after a volume change (ΔV) can be calculated from

$$P_{gauge} = -P_{atm}\left(\frac{\Delta V}{V_{total}+\Delta V}\right), \tag{5}$$

where ΔV is positive for increase in volume.

The generated pressure from the proposed pump agreed quite well with Eq. (5) [Fig. 2(a)], with a maximum error less than 6% and always in the direction of increasing the absolute value of the generated pressure. This error was possibly produced by the increase in air temperature due to the heat generated from the friction between the syringe plunger and its barrel, which deviates from the isothermal process assumption of Eq. (4). This was clearly demonstrated when we tested the system hysteresis, which showed a total increase in the system pressure when the plunger returned to its original starting point (supplementary material, Fig. S1).[22] Heat generation and corresponding pressure error can be mitigated by choosing a proper tank or syringe size to allow for generating the required pressure with shorter plunger displacement. Nonetheless, the changes in air temperature due to plunger friction had negligible effects on the generated pressure at typical pressure ranges required for microfluidic applications.

Generated pressures were highly reproducible [largest standard deviation in Fig. 2(a) is ±600 Pa], suggesting that the integration of a pressure sensor into the system is not crucial since the required pressures can be generated with high accuracy (less than 6% error) by calculating the corresponding values of V_{total} and ΔV. The system can also support applications requiring instantaneous changes in pressure (e.g., micropipet aspiration) with both the resolution and pressure range adjustable by choosing the right tank volume and syringe size (which specifies the smallest achievable volume change ΔV). With a 1 ml syringe (0.01 ml divisions) and a tank volume of 1 l (a water bottle), a resolution of 1 Pa is achieved.

Although the proposed pump generates constant pressures rather than constant flow rates, which are more commonly used in microfluidic applications, desired flow rates can still be accu-

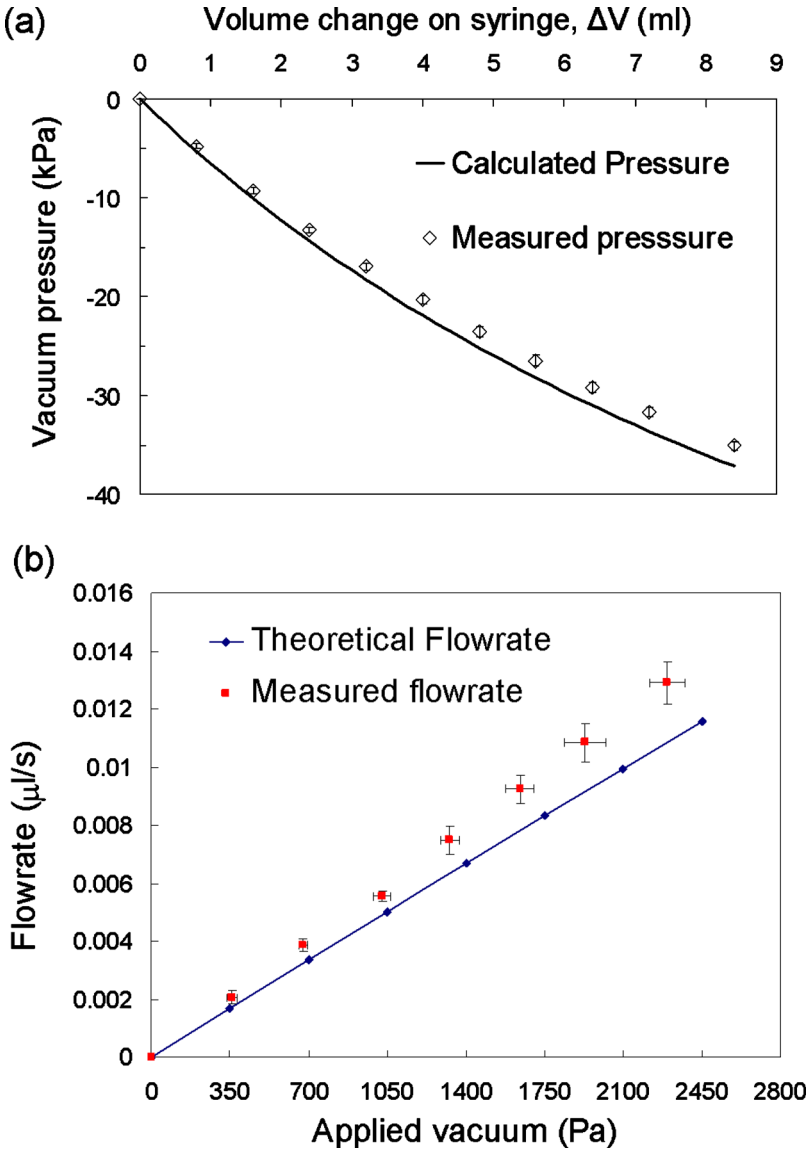

FIG. 2. Pump performance. (a) Vacuum pressure range of −35 kPa with a resolution of 0.9 kPa. Error bars appear inside data markers and present ±1 standard deviation. (b) Flow rate inside a microchannel vs applied pressure. Blue marks represent theoretically calculated flow rates, according to Eq. (6), from vacuum pressures generated by induced volume changes on the syringe, according to Eq. (5). Red marks are actual flow rates measured inside the microchannel. Horizontal error bars represent ±1 standard deviation in the generated pressure, whereas vertical error bars represents ±1 standard deviation in measured flow rate.

rately and easily generated. In microfluidic devices, where laminar flow is dominant, flow rates are linearly proportional to the applied pressures according to Eq. (6) (Ref. 23),

$$Q = \frac{\pi D_h^4}{2C\mu L}\Delta P, \tag{6}$$

where Q is the flow rate, ΔP is the pressure difference between microchannel ends, D_h is the hydraulic diameter of the microchannel connecting the two reservoirs, μ is the liquid viscosity, L is the channel length, and C is a constant depending on the channel cross section ($C=64$ for circular channels, and $C=78$ for channels we tested).[23] This means that any desired flow rate can

TABLE I. Comparison between the performance of our system and other conventional micropumping techniques. Data for other pumping techniques were obtained from Refs. 33 and 8.

Type	Actuation method	Pressure range (kPa)[a]	Maximum resolution (Pa)[a]	Maximum flow rate (μl/min mm^2) [a]	Voltage needed, electrical power (V, W min/ml)[a]
Vibrating diaphragm	Electromagnetic, piezoelectric, magnetic, etc.	920	Not reported	1446	400, 0.938
Peristaltic	Thermopneumatic, piezoelectric	3.5	Not reported	2.14	100, 10.9
Fluid displacement	Magnetic fluid, gas permeation, phase change	2.5	Not reported	0.92	3.4, 2961.5
Rotary	Magnetic or viscous	8	Not reported	601.2	6, 7
Electroosmotic	dc or ac voltage	10 000	Not reported	191.0	6000, 514.7
Syringe pump[b]	dc voltage	~207 (30 psi)	Not reported	35 ml/h	Standard power outlet
Our system	**Manual**	**−95 to 300**	**1**	**4260**[c]	**No electrical power needed**

[a]Values presented are the largest reported with the pumping method.
[b]Flow rate independent of cross section of channel (up to specification limit due to resistance from smaller microfluidic channels). Maximum flow rate and pressure depend on syringe size. Number shown is for 60 cm^3 syringe. Numbers are from New Era Pump Systems INC (http://www.syringepump.com).
[c]Number shown is for a channel of 10 cm length. Flow rate varies with pressure and channel geometry by Eq. (6).

be translated to a pressure difference, which can be directly generated using the proposed pump [Fig. 2(b)]. An advantage of using constant pressures to generate desired flow rates is the absence of the pulsating flow phenomenon as in the use of syringe pumps[10] since flow is generated due to a constant pressure rather than a frictional plunger movement driven by a stepper motor as in syringe pumps.

Since the tubing and syringe in the proposed pump are not filled with the liquid being pumped, the system have zero dead volume, which is defined herein as the volume of liquid left over in the syringe and tubing. At the beginning of an experiment, the amount of liquid desired to be pumped is sucked into the free end of the tubing before it is connected to a microfluidic device. All liquid aspirated into the tubing can be pumped into the microfluidic device.

Since liquid volumes pumped in microfluidic devices are typically of the order of microliters, the displacement of the liquid will not realistically change the volume of the air trapped inside the system; thus, the pressure applied will remain constant throughout the pumping process. Nonetheless, the pump can still deliver large liquid volumes for relevant applications by properly choosing tank volume and syringe size. For example, using a 500 ml tank (e.g., a small water bottle) and a 60 ml syringe, liquid volumes as large as 5 ml can be discharged with a change in pressure less than 10%.

The flow rate generated in microchannels using the new pump followed Eq. (6) satisfactorily with a maximum error of 11% [Fig. 2(b)]. This error in flow rate combines both the error in the generated pressure discussed above and the error in flow measurement, which was performed by tracing fluorescent beads flowing inside the channel. As expected, flow rate was steady throughout the pumping process and did not exhibit any pulsatile behavior.

When compared to existing micropumping methods, our pump demonstrated competitive performance in terms of pressure range, resolution, and flow rate as summarized in Table I. Being electrical power free and being of low cost are additional advantages of the system.

A. Micropipet aspiration

Micropipet aspiration is a common technique used for mechanical characterization of single cells, which could be used as a biomarker for the onset of some diseases such as malaria, sickle

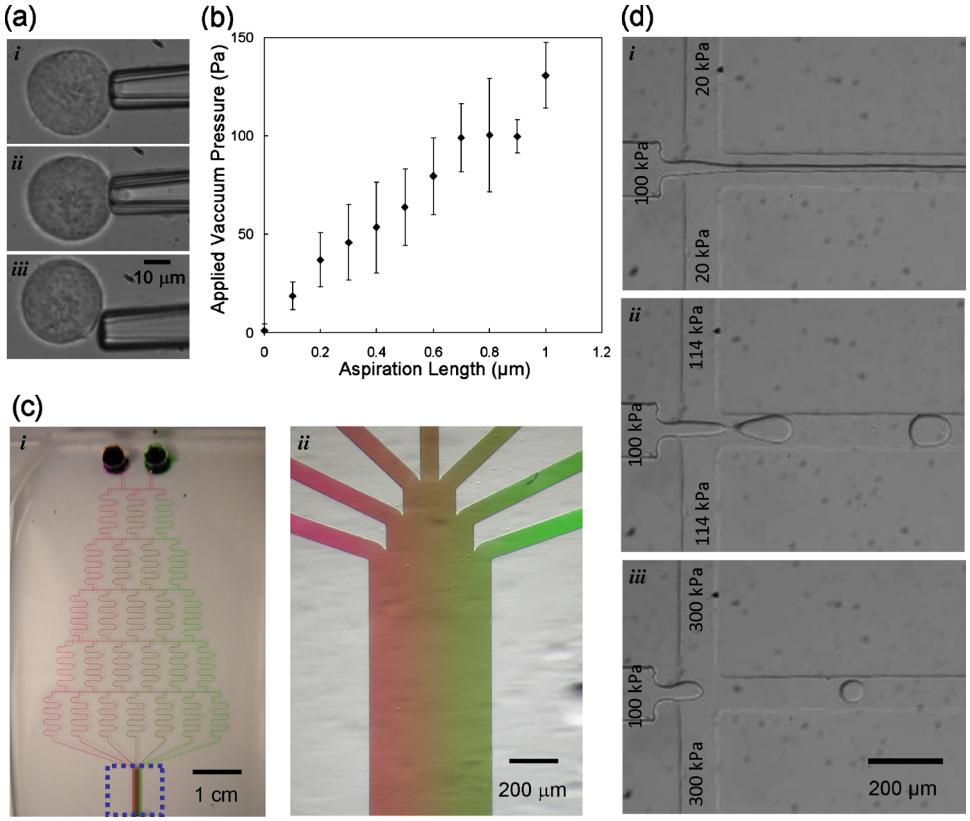

FIG. 3. (a) Video frames (top to bottom) depicting micropipet aspiration and release of an MC3T3-E1 cell. (b) Variation of the cell aspiration length inside the micropipette against applied vacuum pressure. Error bars are ±1 standard deviation ($n=10$ cells). (c) Generating a concentration gradient using two food dyes (red and green). (i) A negative pressure of 15 kPa was applied at the outlet (marked with a dashed box). (ii) Zoomed-in view of the output channel showing the gradient generated. (d) Generation of water droplets in a continuous phase of silicone oil inside a cross-shaped microchannel. Values of applied pressure on each inlet branch are indicated on the three panels.

cell anemia, and cancer.[19] In micropipet aspiration, a micropipet (few microns in diameter) is positioned adjacent to the cell, and a light vacuum pressure (in the order of hundreds of pascals) is applied such that the cell is aspirated into the micropipet. The elongation of the cell into the pipet due to the suction pressure is used, along with the pressure applied, to determine the Young's modulus of the cell.[19,24]

We used the proposed pump to aspirate osteoblasts (MC3T3-E1 cells) into micropipets to calculate its Young's modulus [Fig. 3(a)]. We used tank and syringe volumes of 120 and 1 ml, respectively, which allowed us to produce a pressure range of 730 Pa with a resolution of 8 Pa. This high resolution permitted fine measurement of the aspiration length under different pressures without lysing the cells [Fig. 3(b)]. The relationship between aspiration length and applied vacuum pressure was linear, as predicted by the half-space model.[18] The Young's Modulus of the osteoblast cells was calculated to be 555 ± 183 Pa ($n=10$ cells), which is in agreement with previously reported values.[25]

B. Generation of a concentration gradient

Generating concentration gradients is important for studying many phenomena such as chemotaxis in cell biology and nucleation and growth of crystals in surface chemistry.[20] The dominance of laminar flow in microfluidic devices made it relatively easy to generate concentration gradients of different shape.[26] We used the new pump to generate a concentration gradient inside a 1300 μm wide channel [Fig. 3(c)]. Instead of applying two equal pressures on the two

reservoirs holding the dyes, we applied a vacuum of 15 kPa (total volume=10 ml and syringe displacement=2 ml) at the device outlet, which generated equal flow rates for both dyes since the hydrodynamic resistances of the device two branches were the same due to device symmetry.[27] Applying vacuum to induce the required flow has the advantage of using one pump to deliver different reagents instead of dedicating one pump for each reagent.

C. Droplet generation

Multiphase flow in microchannels offers a new set of advantages besides those seen in single phase flow, such as faster mixing, enhanced heat and mass transfer, and reduced dispersion.[28] Additionally, droplet generation in microfluidic devices has been used for single cell analysis,[4,29] electrophoretic separation,[30] and DNA analysis.[31] To further demonstrate the capabilities of the pump, we used it to generate water droplets in a continuous phase of silicone oil through hydrodynamic focusing of a stream of water in a cross-shaped microchannel [Fig. 3(d)]. Droplet size in our experiments was easily controlled by changing the pressure applied on (and hence the flow rate of) the oil phase as seen in panels ii and iii of Fig. 3(d). Using the same hydrodynamic focusing device, we were able to focus a stream of a miscible dye (supplementary material, Fig. S2),[22] which is useful in various microfluidic applications such as selective delivery of small molecules into biological cells[6] and low-voltage electroporation of cells.[32]

IV. CONCLUSION

The pressure-driven pumping system presented in this paper does not require electrical power. It costs less than $50 without a pressure sensor or $150 with a pressure sensor and can be built within a few minutes from off-the-shelf components. The pump is capable of accurately generating a wide range of positive and negative pressures with high resolutions for microfluidic applications. The use of constant pressures to generate flows in microfluidic devices, instead of displacement pumps (e.g., syringe pumps), has the advantages of zero dead volumes, smooth continuous flow rates, and being compatible with pressure-sensitive applications such as micropipet aspiration and mechanical stimulation of cells. The capacity of the pump was demonstrated by performing micropipet aspiration of osteoblasts to determine their Young's modulus values, realizing a concentration gradient, and generating microdroplets of water in a continuous oil phase.

ACKNOWLEDGMENTS

We thank Jason Li for culturing the MC3T3-E1 cells, Di Xue for helping with flow measurement experiments, and Chris Moraes for supplying the fluorescence beads. We also thank Chris Moraes, Professor Axel Gunther, and Dr. Edmond Young (from Professor David Beebe's laboratory at the University of Wisconsin at Madison) for helpful discussions.

[1] E. W. K. Young and D. J. Beebe, Chem. Soc. Rev. **39**, 1036 (2010).
[2] D. Wu, J. Qin, and B. Lin, J. Chromatogr. A **1184**, 542 (2008).
[3] A. T. Woolley, D. Hadley, P. Landre, A. J. DeMello, R. A. Mathies, and M. A. Northrup, Anal. Chem. **68**, 4081 (1996).
[4] J. F. Edd, D. Di Carlo, K. J. Humphry, S. Köster, D. Irimia, D. A. Weitz, and M. Toner, Lab Chip **8**, 1262 (2008).
[5] S. Nagrath, L. V. Sequist, S. Maheswaran, D. W. Bell, D. Irimia, L. Ulkus, M. R. Smith, E. L. Kwak, S. Digumarthy, A. Muzikansky, P. Ryan, U. J. Balis, R. G. Tompkins, D. A. Haber, and M. Toner, Nature (London) **450**, 1235 (2007).
[6] F. Wang, H. Wang, J. Wang, H. Y. Wang, P. L. Rummel, S. V. Garimella, and C. Lu, Biotechnol. Bioeng. **100**, 150 (2008).
[7] S. A. Khan, A. Gunther, M. A. Schmidt, and K. F. Jensen, Langmuir **20**, 8604 (2004).
[8] B. D. Iverson and S. V. Garimella, Microfluid. Nanofluid. **5**, 145 (2008).
[9] S. Arulanandam and D. Li, Colloids Surf., A **161**, 89 (2000).
[10] R. Yokokawa, T. Saika, T. Nakayama, H. Fujita, and S. Konishi, Lab Chip **6**, 1062 (2006).
[11] D. Dendukuri, S. S. Gu, D. C. Pregibon, T. A. Hatton, and P. S. Doyle, Lab Chip **7**, 818 (2007).
[12] H. V. Fuentes and A. T. Woolley, Lab Chip **7**, 1524 (2007).
[13] J. W. Munyan, H. V. Fuentes, M. Draper, R. T. Kelly, and A. T. Woolley, Lab Chip **3**, 217 (2003).
[14] C. C. Hong, J. W. Choi, and C. H. Ahn, J. Micromech. Microeng. **17**, 410 (2007).
[15] G. M. Walker and D. J. Beebe, Lab Chip **2**, 131 (2002).
[16] A. M. Skelley and J. Voldman, Lab Chip **8**, 1733 (2008).
[17] R. K. Shah and A. L. London, *Laminar Flow Forced Convection in Ducts; A Source Book for Compact Heat Exchanger Analytical Data* (Academic, New York, 1978).

[18] D. P. Theret, M. J. Levesque, M. Sato, R. M. Nerem, and L. T. Wheeler, J. Biomech. Eng. **110**, 190 (1988).
[19] C. T. Lim, E. H. Zhou, and S. T. Quek, J. Biomech. **39**, 195 (2006).
[20] N. L. Jeon, S. K. W. Dertinger, D. T. Chiu, I. S. Choi, A. D. Stroock, and G. M. Whitesides, Langmuir **16**, 8311 (2000).
[21] H. Kim, D. Luo, D. Link, D. A. Weitz, M. Marquez, and Z. Cheng, Appl. Phys. Lett. **91**, 133106 (2007).
[22] See supplementary material at http://dx.doi.org/10.1063/1.3499939 for measurments of the pump hysteresis and results of a hydrodynamic focusing experiment using the proposed pump.
[23] B. R. Munson, D. F. Young, and T. H. Okiishi, *Fundamentals of Fluid Mechanics*, 4th ed. (Wiley, New York, 2002).
[24] R. M. Hochmuth, J. Biomech. **33**, 15 (2000).
[25] E. Takai, K. D. Costa, A. Shaheen, C. T. Hung, and X. E. Guo, Ann. Biomed. Eng. **33**, 963 (2005).
[26] S. K. W. Dertinger, D. T. Chiu, J. Noo Li, and G. M. Whitesides, Anal. Chem. **73**, 1240 (2001).
[27] T. Stiles, R. Fallon, T. Vestad, J. Oakey, D. W. M. Marr, J. Squier, and R. Jimenez, Microfluid. Nanofluid. **1**, 280 (2005).
[28] A. Günther and K. F. Jensen, Lab Chip **6**, 1487 (2006).
[29] M. Y. He, J. S. Edgar, G. D. M. Jeffries, R. M. Lorenz, J. P. Shelby, and D. T. Chiu, Anal. Chem. **77**, 1539 (2005).
[30] J. S. Edgar, C. P. Pabbati, R. M. Lorenz, M. He, G. S. Fiorini, and D. T. Chiu, Anal. Chem. **78**, 6948 (2006).
[31] M. A. Burns, B. N. Johnson, S. N. Brahmasandra, K. Handique, J. R. Webster, M. Krishnan, T. S. Sammarco, P. M. Man, D. Jones, D. Heldsinger, C. H. Mastrangelo, and D. T. Burke, Science **282**, 484 (1998).
[32] T. Zhu, C. Luo, J. Huang, C. Xiong, Q. Ouyang, and J. Fang, Biomed. Microdevices **12**, 35 (2010).
[33] D. J. Laser and J. G. Santiago, J. Micromech. Microeng. **14**, R35 (2004).